Engineering and Technology Journal
Journal homepage: https://etj.uotechnology.edu.iq

Enhancing the removal of total dissolved solids from petroleum wastewater through electrocoagulation

Muhammad A. Jasim[a], Forat Yasir AlJaberi[b,c*], Saja M. Alardhi[d], Ali D. Salman[e], Mustafa M. Hathal[f], Igor Cretescu[g], Armando R. Vargas[h]**

[a] Samawa Refinery Department, Board of Production, Midland Refineries Company, Ministry of Oil, Al-Muthanna, Iraq.
[b] Chemical Engineering Department, College of Engineering, Al-Muthanna University, Al-Muthanna, Iraq.
[c] College of Engineering, Al-Ayen University, Thi-Qar, Iraq.
[d] Nanotechnology and Advanced Material Research Center, University of Technology, Iraq.
[e] Department of Chemical Engineering, College of Engineering, University of Baghdad, Aljadria, Baghdad, Iraq.
[f] Sustainability Solutions Research Lab, Faculty of Engineering, University of Pannonia,gyetem Str. 10, Veszprém H 8200, Hungary.
[g] Department of Environmental Engineering and Management, Gheorghe Asachi Technical University of Iasi, Romania.
[h] Industrial Engineering Department, Universidad of Holguín, Cuba.
*Corresponding author Email: furat_yasir@yahoo.com ;**Corresponding author Email: 11659@uotechnology.edu.iq

HIGHLIGHTS

- Aluminum ions release from the anode faster than hydroxyl ions from the cathode.
- An innovative reactor from a local factory is used to reduce TDS in petroleum effluent.
- Box-Behnken Design and Minitab optimized experimental design, analysis, and variables.
- longer electrolysis durations and higher current densities led to decreased TDS levels.

Keywords:

Petroleum effluent

Total dissolved solids

Electrocoagulation process

Electrodes consumption

Finned cathode tube

ABSTRACT

This study aims to employ an electrocoagulation reactor to treat petroleum effluent from a local plant and reduce dissolved solids (TDS) to suitable levels for reuse. A continuous reactor configuration featured a finned stainless steel cathode tube positioned between two cylindrical aluminum anodes. This study explored the influence of treatment duration (4–60 minutes), current density (0–6.0 $mA.cm^{-2}$), and influent rate (50–150 ml/min) on the final TDS value. Flow rate increase correlated with increased final TDS values, while longer electrolysis durations and higher current densities led to decreased TDS levels. Optimized electrolysis conditions at 1 hour, 5 $mA.cm^{-2}$, and 50 ml/min, with inner and outer anode consumptions of 0.18 g and 0.45 g, respectively, achieved a final TDS of 2000.45 mg/l, representing a reduction of 207.55 mg/l. The regression model, with a p-value of 0.0001, F-value of 219.37, and R2 of 99.75%, demonstrated the significance of the model components, indicating its robustness. The energy consumption was 3.65 kWh/m^3, and the total operating cost was only 0.74 $ per m^3. This study confirms the efficacy of the novel continuous reactor in managing petroleum wastewater under practical conditions with low consumption values of electrodes and electrical energy.

1. Introduction

Crude oil undergoes various refining processes in petroleum refinery plants to yield valuable products such as kerosene and gasoline. Throughout these operations, oily wastewater is generated, notably in units like desalters, condensate systems, hydrocrackers, and condensate flares [1]. The refining of crude oil is water-intensive, resulting in significant wastewater production [2]. Crude oil itself comprises a complex mixture of organic (hydrocarbons) and inorganic components (including turbidity, Total Dissolved Solids (TDS), Chemical Oxygen Demand (COD), Total Suspended Solids (TSS), ammonia (NH_3), arsenic (As), and various toxic metals) [3, 4]. The water content in crude oil can vary depending on factors such as well depth and location, consequently leading to the discharge of oily effluents, a primary contributor to marine ecological pollution [5]. Due to the persistent nature of oily wastewater, its presence poses significant challenges to both environmental and human health [6-8]. Hence, depending on the composition and volume of emulsified oily wastes, diverse treatment methodologies are required to address effluent sources effectively.

Al-Muthanna petroleum refinery has a daily capacity of 30000 barrels. The water content in crude oil from oil fields is 0.2 ppm, consumes 3.2 cubic meters of fresh water per hour per thousand barrels of crude oil in the desalter unit and 1.5 cubic meters

http://doi.org/10.30684/etj.2025.157123.1893
Received 01 February 2025; Received in revised form 21 February 2025; Accepted 07 March 2025; Available online 19 March 2025
2412-0758/University of Technology-Iraq, Baghdad, Iraq

of fresh water per hour per thousand barrels of crude oil in the refinery units (distillation tower, stripper tower, and other services). The amount of wastewater discharged is 4 cubic meters per hour. The basic treatment techniques used to accomplish this goal include adsorption, cyclone separation, chemical precipitation, and electrochemical approaches [9]. The effectiveness of the employed techniques is influenced by their capacity for elimination, time required to finish the treatment, additional pollutants produced, construction cost, and operation/maintenance costs [10]. Therefore, to remove organic and inorganic components from wastewater and allow freshwater reuse, some skillful treatment techniques are required due to the quick development of industries and human needs [11].

Physical, chemical, and mechanical processes are used to treat these effluents, ordinarily accompanied by biological processes [12]. Mechanical and physical treatments include gravitational or centrifugal separations, membrane filtration, flotation, and others. These classic procedures can remove solid particles, emulsified oil, and free oil in suspension from wastewater [13].

The biological process is effective in reducing biochemical oxygen demand (BOD). However, when very toxic recalcitrant contaminants, such as the aromatic part of dissolved organic compounds, are present in wastewater, employing the biological process is insufficient [14,15]. Furthermore, previous approaches have revealed various operational issues such as energy consumption, partial effluent degradation, secondary phase creation, and toxic intermediates synthesis, all of which impose additional costs on the process. Innovative approaches should be used to remove these harmful contaminants in this case [16, 17]. Adsorption is one of the most effective wastewater treatment procedures for reducing organic and inorganic chemicals that remain in effluents after conventional treatment. The most extensively used approach is adsorption using activated carbon, which requires prohibitively expensive adsorbents [18].

In recent years, electrochemical wastewater treatment technologies have received a lot of attention [19-21]. These methods include electro-oxidation, electro-fenton, and electro-coagulation (EC), as well as their sequential and concurrent combinations, for the treatment of industrial wastewater [22-24]. Electro-fenton is a revolutionary variation of the traditional Fenton method for the elimination of organic contaminants. A high level of contaminant eradication is achieved in this procedure by using Fenton's reagents and anodic oxidation [25, 26].

EC can avoid using excessive coagulant ingredients by treating wastewater with electricity [27]. It was proposed for the first time in the United Kingdom in 1889. In “1904” Elmore was the first to propose the use of electrolysis in mineral extraction [28]. The EC process is an eco-friendly, effective, speedy, and economical remediation for the removal of various toxicants, such as dissolved metals, tannin, phenol, and COD, from water and wastewater [29, 30]. A comparison topic between the electrochemical method and other conventional methods is shown in Table 1:

Table 1: A comparison between electrochemical technologies and another treatment method

Treatment methods	Advantages	Disadvantages
Adsorption	Applicable for a wide range of the pH Easy operating conditions	Generation of waste products Low selectivity
Chemical precipitation	Not complex operation Capital cost is low	Additional cost needed to disposal the huge sludge
Membrane filtration	High selectivity Space requirement is not large	Membrane fouling requires High operating cost
Ion exchange	Convenient operations	Too expensive Highly sensitive to the pH value of the solution
Electro-coagulation	The tool's affordability, simplicity, and ease of use. Because there are no moving parts needed and the process is electrically controlled, minimal maintenance is needed. It can be powered by wind or solar energy. Easy to collect, dehydrate, filter, and separate; low EC sludge production. Chemical coagulants are unnecessary since they will result in secondary contamination. The cathode electrodes' emission of hydrogen gas during the remediation procedure. These bubbles aid in the collection and removal of contaminants by bringing them to the top of the treated water.	Electrical energy consumption, which limits its utilization and raises operating expenses. During the anode oxidation process, an oxide layer may form on the electrode surfaces, decreasing the removal effectiveness. The anode electrodes need to be changed on a regular basis due to the high conductivity of the solutions, which causes their consumption to rise quickly.

EC is a simple and efficacious method for treating different kinds of wastewater that has had great success in eliminating the majority of pollutants [31]. The EC mechanism is based on the decomposition process, which releases so many ions from the anode and cathode. Through the adsorption process, contaminants are eliminated because aluminum ions (in the case of aluminum electrodes) react with hydroxyl ions to generate electro-coagulants [32, 33]. Typically, iron or aluminum serves as the anode and cathode, negating the need for chemical additives. For the last three decades, EC has been applied as a successful water-remediation technology to remove a wide range of pollutants [34, 35]. As the electric current passes through the EC cell, redox reactions proceed at both electrodes. According to water analysis, the anode's surface produces Al^{3+} ions due to the oxidation process of the anode. These ions combine with the cathode's OH^- ions that are produced based on the reduction process to generate solid $Al(OH)_3$ coagulants [18]. Oxygen and hydrogen gases emitted from the anode and cathode, respectively, will

encourage the flotation process of lighter pollutants toward the surface of a liquid. With the help of adsorption, electro-coagulants created from the ions produced by the two electrodes will remove pollutants efficiently [19, 22].

Aluminum ions are released from the anode much more frequently than hydroxyl ions released from the cathode because the oxidation process in the electrochemical cell typically proceeds more quickly than the reduction process. To increase the reactor's capacity, the cathode's surface area should be increased. Fins on either side of the cathode's surface and a reactor with a relatively low wet volume were used in this work to address this problem. More hydroxyl ions and aluminum ions from finned-cathode and tubular anodes, respectively, will increase the production of $Al(OH)_3$ coagulants and consequently enhance pollution removal efficiency.

This project will utilize this innovative reactor to decrease the TDS presented in petroleum effluent released from a local petroleum factory. The experimental design, result analysis, and operational variable optimization were conducted utilizing the Box-Behnken Design (BBD) methodology and Minitab software.

2. Materials and methods

2.1 Petroleum wastewater collection

Petroleum wastewater utilized in this study was collected from the Al-Muthanna petroleum refinery's effluent discharge point Table 2, with an approximate daily flow rate of 96 m^3, and subsequently processed in a continuous EC reactor.

Table 2: Petroleum wastewater characterization

Variables	TDS [mg/l]	pH [-]	Conductivity [ms/cm]	(OC) [mg/l]
Amounts	2208	7.9	4.370	1466.8

Equation 1 below is used to compute the actual electrode consumption (ACE) during the continuous EC process [5, 36]:

$$\text{Actual Consumption of Electrodes (AEC)} = w_1 - w_2 \quad (1)$$

w_1 stands for the electrode mass prior to testing, and w_2 for the electrode mass following testing [37].

Equations (2 and 3) are conducted to calculate the values of electrical energy consumption in (kwh/m^3) and total operating cost in (\$/m^3), as follows:

$$\text{Econs} = (U.I.t)/(1000.V) \quad (2)$$

$$\text{Total operating cost} = a \times AEC + b \times \text{Econs} \quad (3)$$

where U refers to the voltage applied (volt), I is the supplied current (Amps.), t is the electrolysis time (h), V refers to the solution volume (m^3), and a and b symbols refer to the price per unit weight of electrode (\$/mg) and unit electric energy price (\$/kW.h) unit electric energy price (\$/kW.h) [equal to 2.74*10-3 \$/mg and 0.013 \$/kW.h at the time of this research], respectively.

2.2 Electrocoagulation reactor design

A direct current supply type (YX-305D, Yaxun-China) was used throughout the experiment to maintain a steady current while permitting voltage fluctuations. There was a 2.5 L plastic EC tank on hand. Three concentric electrode tubes were employed in an EC reactor for this experiment. Figure 1 (a and b) depicts the electrode configuration and the procedure of the EC treatment. On the basis of that initial hypothesis, the current analysis identified a novel electrode configuration design Table 3.

Table 3: Dimensions of electrodes used in this study

Parameters	Height (cm)	Outer diameter (cm)	Fin Height (cm)	No. of Fins	Wet height (cm)
Inner Anode (Aluminum)	10	1.5	-	-	7.5
Cathode (Stainless steel)	10	5	10	6	7.5
Outer Anode (Aluminum)	10	12	-	-	7.5

The overall immersed surface area of the anode was 319 cm^2. The inside and outside anodes were separated from the cathode by 1 cm and 2 cm, respectively, and were connected to the direct current (DC) electricity source. Two-Side Finned (2SF) stainless steel with longitudinal fins on both sides serves as the cathode in this study. The six interior fins had a diameter of 1 cm, a height of 10, and a thickness of 0.3 cm, while the six outside fins had a diameter of 2 cm, a height of 10, and a thickness of 0.3 cm. The surface area of the entire structure was 667 cm^2.

Generally speaking, the electrochemical cell's oxidation process is quicker than its reduction process. This implies that the anode releases aluminum ions more quickly than the cathode releases hydroxyl ions. For this reason, the cathode's surface area must be optimized without unduly increasing the reactor's volume. This work used fins on both sides of the cathode's surface with a remarkably small reactor wet volume in an attempt to solve this problem. More electro-coagulants containing aluminum ions will be produced as a result of the increased hydroxyl ion content, and higher pollution removal efficiency may be achieved as a result.

After each experiment, the electrodes were cleaned and washed with distilled water, allowed to dry, and then weighed to determine the amount of consumption. TDS concentrations were also measured. In this study, the analyzed indices were TDS. The TDS of petroleum wastewater was calculated using a conductivity meter of ions (HM DIGITAL-Korea).

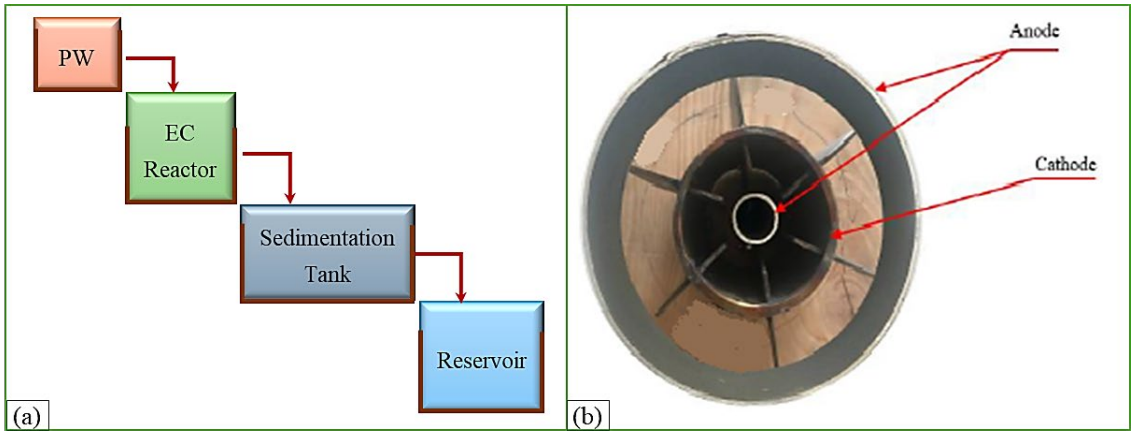

Figure 1: (a) The procedure of the present EC and (b) how the electrodes are positioned

2.3 Experimental design planning

The EC experiments were devised, assessed, and refined using Minitab-18 along with the Box-Behnken Design (BBD). By incorporating the desired response into a second-order polynomial Equation, Equation 2 serves to establish the mathematical relationship between the responses and the operational variables. The degree to which the model accurately reflects reality hinges on the regression coefficient value (R2) and the analysis of variance (ANOVA) feedback [38, 39].

$$Y = B_0 + \sum_{i=1}^{q} B_i X_i + \sum_{i=1}^{q} B_{ii} X_i^2 + \sum_i \sum_j B_{ij} X_i X_j + \varepsilon \quad (2)$$

In this equation, Y represents the final TDS value, where q stands for all of the operational parameters, X1 to Xq denotes the operating factors, and the coefficient vectors range from B0 to Bij. The present study investigated CD (X1: 0.63–5.0 mA.cm^{-2}), electrolysis time (X2: 4-60 minutes), and flow rate (X3: 50-150 ml.min^{-1}). Design specialists recommended 12 trial investigations utilizing 3 centroids, specifically employing BBD, to optimize the identified response. The explored solutions are represented as Y in terms of the Final TDS value, where q stands for all of the operational parameters, The operating factors range from X1 to Xq, and the coefficient vectors range from Bo to Bij. The current study investigated CD current density (X1: 0.63–5.0 mA.cm^{-2}), electrolysis time (X2: 4-60 minutes), and flow rate (X3: 50-150 ml.min^{-1}). Design specialists suggested 12 trial investigations using 3 centroids, particularly using RSM-BBD, to improve the identified response.

3. Results and discussion

Table 4 displays the operational factors' actual values as well as the experimental and anticipated final TDS levels for the inner and outer tubular electrodes. Figure 2 displays the observed results of the final (TDS) as dots along the fitted line. The final TDS predicted values, as a result of this, significantly deviate from the fitted line. The difference between the experimental and predicted TDS levels shows that random error is minimal. Positive residuals are indicated by dots above this line, indicating that the expected values are more than the observed values. The residual is negative if any dots fall below this line, suggesting that the results are poorer than what was actually seen.

Table 4: The main results of the studied variables

Run	X1: CD (mA/cm^2)	X2: Electrolysis time (min)	X3: Flow rate (ml/min)	Experimental TDS (mg/l)	Predicted TDS (mg/l)	Inner Anode Consumption (g)	Outer Anode Consumption (g)
1	0.630	4	100	2206	2211	0.001	0.01
2	5.000	4	100	2210	2209	0.001	0.01
3	0.630	60	100	2181	2182	0.02	0.13
4	5.000	60	100	2071	2066	0.07	0.17
5	0.630	32	50	2200	2197	0.03	0.08
6	5.000	32	50	2133	2136	0.02	0.15
7	0.630	32	150	2273	2270	0.02	0.07
8	5.000	32	150	2210	2213	0.03	0.12
9	2.815	4	50	2250	2248	0.001	0.02
10	2.815	60	50	2040	2042	0.05	0.27
11	2.815	4	150	2206	2204	0.001	0.02
12	2.815	60	150	2237	2238	0.02	0.13
13	2.815	32	100	2149	2153	0.03	0.18
14	2.815	32	100	2153	2153	0.04	0.18
15	2.815	32	100	2158	2153	0.03	0.18

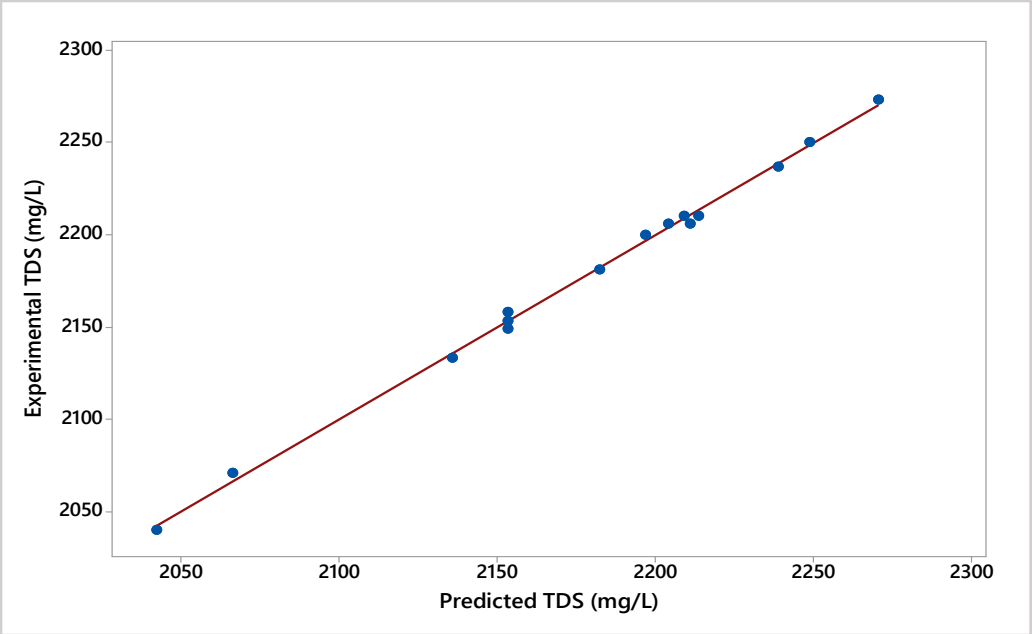

Figure 2: Final TDS experimental and predicted values

3.1 Mathematical relationship of investigated responses

Analyzing the relationships among operational factors in relation to key parameters enables the prediction of final TDS based on experimental data utilizing the mathematical correlation Equation 3. Assessing the model fit relies on peak regression factor values and the alignment between variable response values and the generated TDS model, with higher regression parameter values indicating a better model fit [40]. As observed, the high values of the regression coefficient R2-adj (0.993) and R2 (0.998) for the studied response variable TDS indicate the excellent fit of the model to the data [5].

$$Y_{TDS\,\%} = 2420.7 - 19.80\,X_1 - 4.234\,X_2 - 3.322\,X_3 + 3.604\,X_1^2 - 0.00452\,X_2^2 + 0.01338\,X_3^2 - 0.4658\,X_1X_2 + 0.0092\,X_1X_3 + 0.04304\,X_2X_3 \quad (R^2 = 0.998;\ R^2\text{-adj} = 0.993) \quad (3)$$

To ensure the model's reliability, analysis of variance (ANOVA) was employed as a key analytical tool [36] (Table 5). Table 5 presents the variance analysis results for the final TDS levels. Certain model components exhibit statistical significance in the proposed models, with p-values less than 0.05. The high F-parameter value of 219.37 for TDS in the current study indicates an excellent fit of the generated model. Moreover, the Lack-of-Fit p-value exceeding 0.05 further supports the accuracy and statistical significance of the generated model. According to the ANOVA results, these models suggest that the EC process effectively removes contaminants from oily wastewater.

Table 5: Results of the final TDS value's ANOVA test

Source	Degree of Freedom	Sum of squares	Mean square	F-Value	P-Value	Remarks
Model	9	56037.8	6226.4	219.37	<0.0001	highly significant
X_1	1	6962.0	6962.0	245.28	<0.0001	highly significant
X_2	1	14706.1	14706.1	518.13	<0.0001	highly significant
X_3	1	11476.1	11476.1	404.33	<0.0001	highly significant
X_1^2	1	1093.4	1093.4	38.52	0.002	Significant
X_2^2	1	46.3	46.3	1.63	0.258	
X_3^2	1	4133.4	4133.4	145.63	<0.0001	highly significant
X_1*X_2	1	3249.0	3249.0	114.47	<0.0001	highly significant
X_1*X_3	1	4.0	4.0	0.14	0.723	
X_2*X_3	1	14520.3	14520.3	511.58	<0.0001	highly significant
Error	5	141.9	28.4			
Lack-of-Fit	3	101.2	33.7	1.66	0.397	
Pure Error	2	40.7	20.3			
Total	14	56179.7				

3.2 Process factors' effects on the final TDS response

3.2.1 Current density's impact

Figure 3 shows how current density affects the final TDS response when the mean values of other factors are taken into consideration. Current density is the most crucial operating variable to take into account during the electrocoagulation process since it affects both the amount of various ions released from electrodes and, as a result, the rate of pollutant removal. Because an electric current is continuously supplied without the need for chemical additives to reduce the amount of TDS, the electrochemical coagulation technique is always reliant on the production of coagulants. The way that TDS responds will be affected by the production of these coagulants in the ECR. As a result, a number of factors, including the electrocoagulation reactor's performance, the electric current used, and the electrode arrangement and active area, might change the TDS concentration [41, 42].

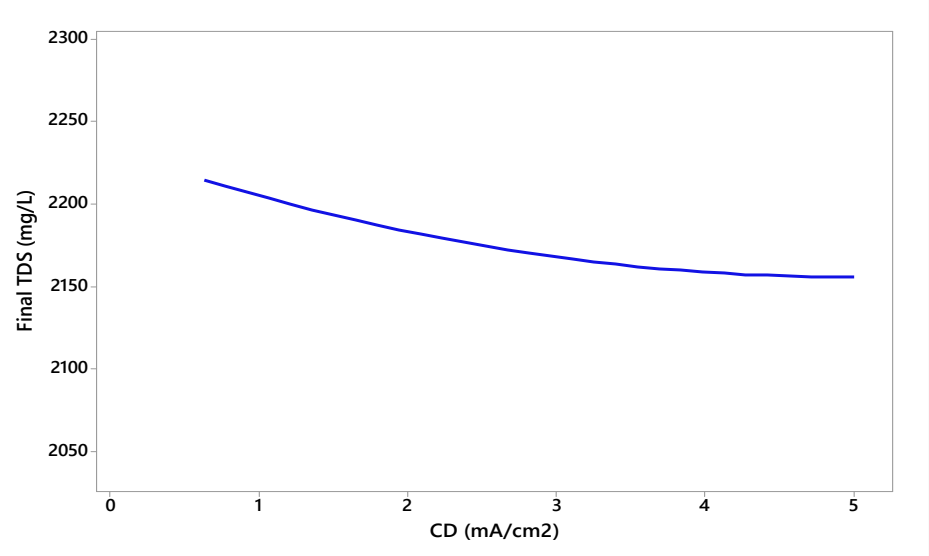

Figure 3: Influence of current density (mA/cm^2) on the final TDS

Figure 3 displays the correlation between the ultimate removal of TDS and CD parameters with an influent rate of 100 ml/min and a mean treatment time of 32 minutes to highlight how current density impacts the efficiency of EC reactors. The results demonstrate that the anode's capacity to produce sufficient adsorbents to eliminate pollutants from wastewater increases as CD increases. The TDS decreased from 2181 ppm at 0.630 mA.cm^{-2} to 2071 ppm at 5.000 mA.cm^{-2}. Additionally, the current design's cathodic active area helped create more hydroxyl ions than were necessary to build more electro-coagulants, which enhanced the removal of TDS [38, 43]. The findings can be explained as the reaction accelerates at high current density levels because the amount of TDS steadily decreases with rising current density. According to Jasim, AlJaberi, Salman, Alardhi, Le, Kulcsár, Jakab [1] and Ganzenko, Huguenot, Van Hullebusch, Esposito, Oturan [22], the efficiency of pollutant removal is now operating similarly to the existing density. The final TDS response to the CD and the average values of other variables are quantitatively illustrated in Equation 4:

$$Y = 1531\,X_1 - 226.7\,X_1^2 \qquad R^2 = 88.5\% \qquad (4)$$

3.2.2 Effects of electrolysis duration

When the mean values of other variables are employed, as shown in Figure 4, we can observe how the electrolysis duration impacts the final TDS response. In Figure 4, a steady decline in the final studied response as the electrolysis duration increases is illustrated. Adsorption typically happens in three sequential steps: first, the contaminant is transported from the solution to the adsorbent surface. Then, it is adsorbed on the surface. Lastly, it is transported within the adsorbent particle. In order to make the adsorption process more active and quick, as well as to reduce the amount of time needed to complete the process, low energy will be used. This is because the anode's dissolution creates anions that are needed to work with opposite ions to form coagulants. The necessary adsorbents for the electrocoagulation process were formed as a result of the constant release of hydroxyl and aluminum ions. As a result, aluminum hydroxyl functions as an effective adsorbent and can remove harmful pollutants from wastewater. The cathode tube's active area on both sides supplies a significant quantity of hydroxyl ions needed to create the adsorbent. The results of this study demonstrate how the continuous supply of current into the electrolytic cell during the reaction time has impacted the continuity of pollutant adsorption through the formation of the adsorbent due to the reaction between aluminum and hydroxyl ions released from the anode's dissolution and the cathode's reduction, independently.

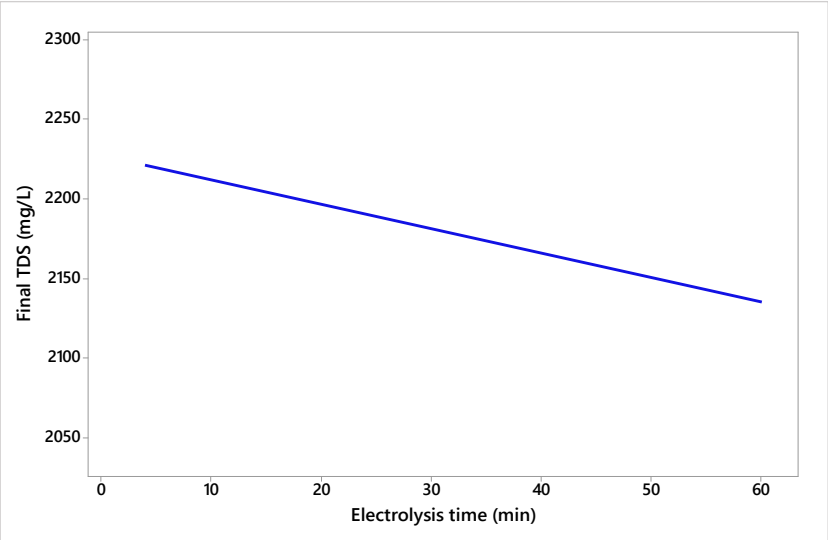

Figure 4: The influence of the electrolysis time on the final TDS

With prolonged designed time, contaminants undergo elimination from the solution through adsorption and desorption processes occurring within the EC cell [27, 44]. Within the EC process, electrostatic interactions among negatively charged particles induce the electro-generation of $Al(OH)_3$ and impurities, leading to hetero-aggregation. This amalgamation of aluminum ion composites and TDS from wastewater results in flocculation. The production of additional aluminum ionic composites necessitates longer reaction times to neutralize the anions in the effluent. Both [6] and [25] reached similar conclusions. Equation 5 establishes the relationship between the TDS response and treatment time when recent variables are at their mean values:

$$Y = 124.4\,X_2 - 1.514X_2^2 \qquad R^2 = 82.2\% \qquad (5)$$

3.2.3 Effect of flow rate

When the mean values of other factors are taken into account, as shown in Figure 5, we can observe how flow rate impacts the final TDS response. The removal of TDS is significantly impacted by the wastewater flow rate, as seen in Figure 5. Changes in the wastewater flow rate affect how long the current electrodes in the EC reactor take to complete an electrolysis cycle. The existing architecture of the chemical reactor allows for continuous operation; hence, the flow rate (50 - 150 ml/min) was the operational factor picked. It has been shown that the TDS behavior changes when the influent rate changes. Because the pollutant reduction process does not give the pollutants enough time to attach to the various ions, they drop when flow rates increase when they are low, but they increase as flow rates increase when they are high. The concentration of contaminants in the reactor will rise as a result of the wastewater's feed increases. In order to accelerate the sedimentation and flotation process, a suitable amount of electro-coagulant is needed to adsorb pollutants to a certain extent and generate a mixture of flocs and pollutants. Additionally, a higher flow rate will result in a shorter residence time for the material inside the reactor (the secondary passage process) and more vortices between the electrodes, which will lessen the destabilization process between the material particles.

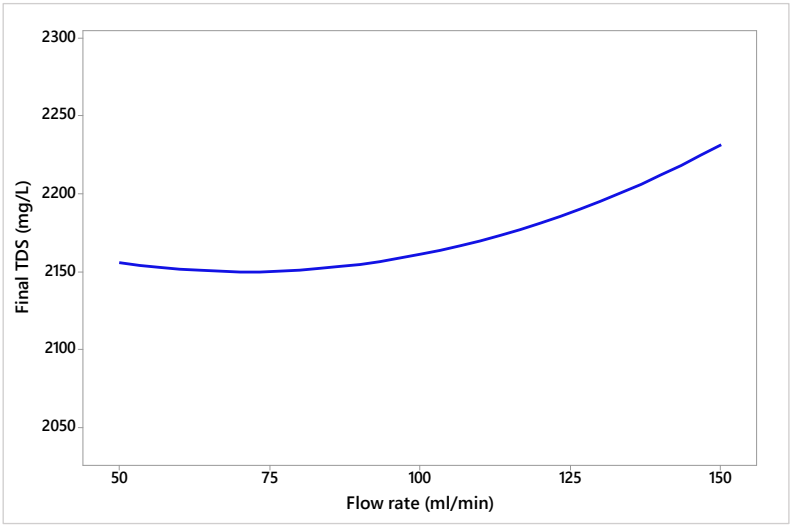

Figure 5: Flow rate's effect on final TDS

Due to this, some of the solutions pass without having an impact on the environment. A similar conclusion was made in [1]. Equation 6 illustrates the quadratic relation between the TDS response and influent rate at the mean values of other variables:

$$Y = 44.56\,X_3 - 0.2044\,X_3^2 \qquad R^2 = 98.1\% \qquad (6)$$

The amount of aluminum ions emitted from the anode is correlated with the TDS value. It depends on length of the electrolysis, the flow rate, and current density how easily aluminum ions dissolve. This demonstrates how the concentration of dissolved solids can change based on how much electrode is actually consumed in addition to the concentration of dissolved salts. The studied response starts to increase at ultimate CD values when the production of Al-ions is high and much greater than the contaminants in the sample, and it rises at high influent rates when the concentration of dissolved salts is high. Figure 6 shows the contour plots indicating each set of operational parameters—current density of 2.815 mA/cm^2, 32 min of the electrolysis time, and 100 ml/min of influent rate—significantly affects the TDS response. While each pair is changed in accordance with the planned range, the other variable is maintained at its typical value for each occurrence. The treatment time-influent rate pair has a substantially greater influence than the CD-treatment period pair and the CD-influent rate pair, based on the behavior of TDS removal displayed in the contour plot. These results closely match the ANOVA test displayed in Table 5.

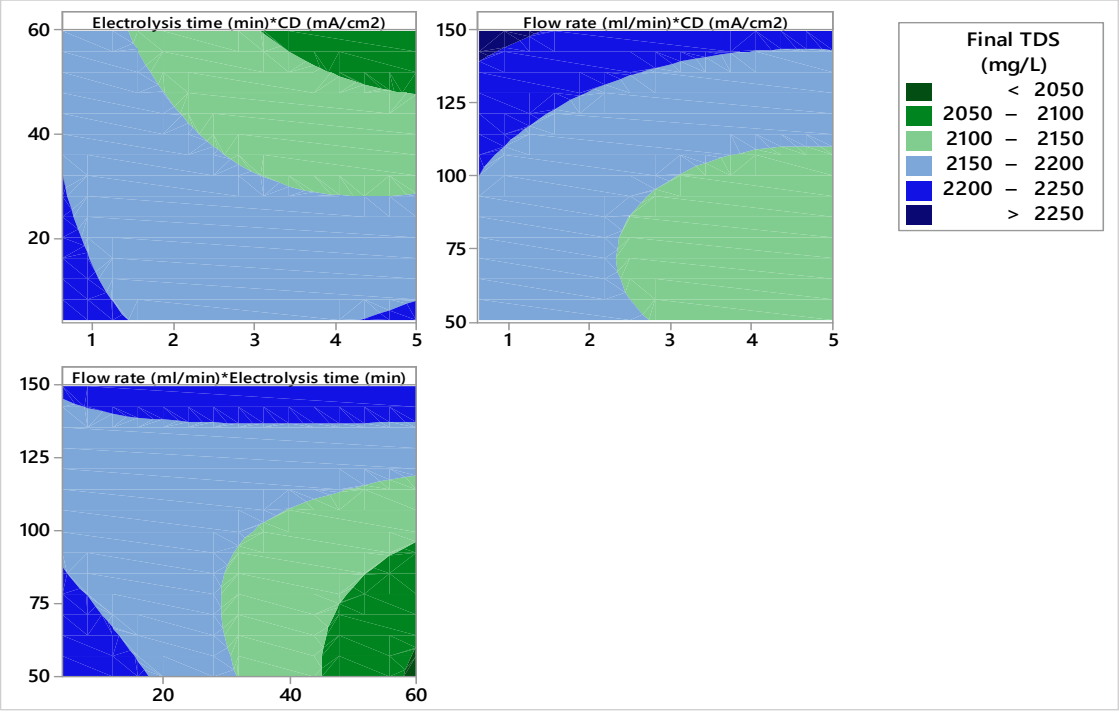

Figure 6: The response of final TDS compared to the analyzed variables' contour plots. (a) Pair of the CD and treatment time (a) Pair of CD and flow rate (b) (c) Pair of treatment time and flow rates

3.3 Electrodes consumption

Because the release of different ions from the electrodes causes higher concentrations of pollutants to demand more adsorbents at the start of the experiment, the results can be explained by the fact that when there is an excess of adsorbents, the dissolution of the electrodes is decreased. The active area provided by the existing design of the innovative electrode and the electrical conductivity of greasy wastewater caused a progressive increase and decrease in the actual electrode consumption. The development of an oxide layer on the anode surface slows the anode decomposition process. As it regulates the pace at which pollutants are eliminated by ions released from the electrodes, electrode consumption is a crucial component of electrocoagulation. Because of the cathode's careful design, which gives it a larger surface area than the outer side due to the presence of fins, the results show that consuming the outer electrode has a greater effect on the final TDS value than consuming the inner electrode. This helps to release a larger amount of hydroxide, which combines with the aluminum ion to form a large amount of adsorbent. To purge a solution of contaminants.

3.3.1 Consumption of inner-anode

For the factors examined, the electrical exhaustion of anodes was determined using Equation 1. Based on Figure 7, the following goals will be investigated to comprehend how process variables impact the consumption response of the inner anode when the mean values of other variables are present:

The findings depicted in Figures 7a and 7b indicate that the inner anode consumption increased with CD but accelerated with longer treatment durations. Upon reaching moderate levels, this response gradually plateaued and eventually declined. Figure 7c illustrates the consumption of the inner anode relative to the influent rate. Initially, influent rates surged before gradually decreasing.

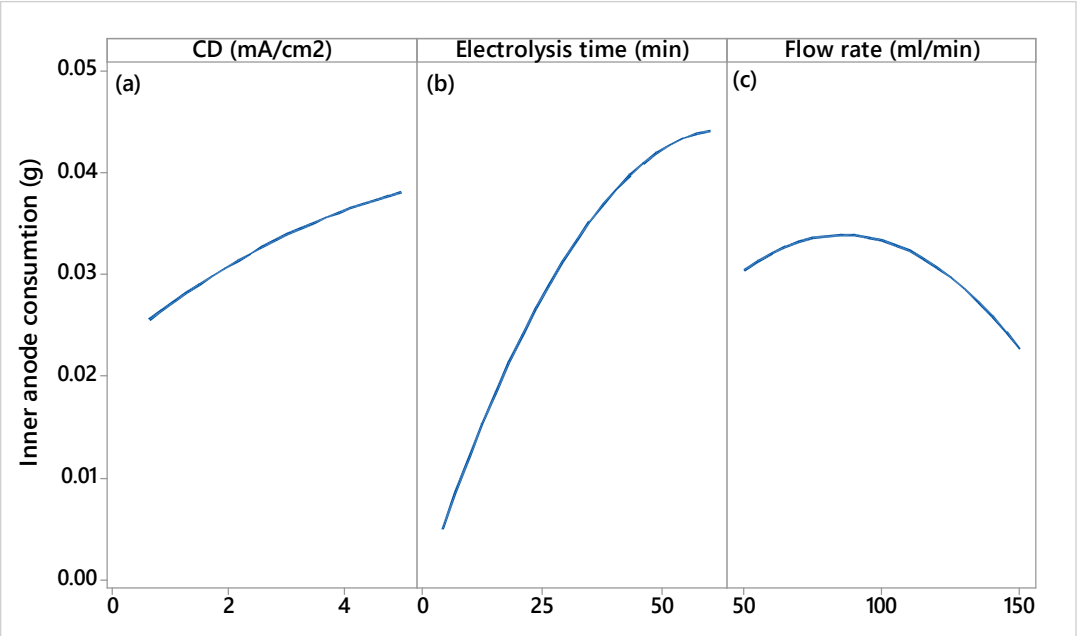

Figure 7: Operating parameter effects on inner-anode consumption. (a) CD (mA/cm^2), (b) The treatment time (min), and (c) The influent rate (ml/min)

3.3.2 Consumption of outer-anode

The following research objectives will be examined in light of Figure 8 in order to ascertain how process parameters affect the response of the consumption of the outer anode in the event of mean values for other operating variables. Figures 8a and 8b illustrate the relationship between the electrolysis time, current density, and the response of the outer anode to consumption. The findings demonstrated that the consumption amount of the outer anode steadily rose as current density did, decreased gradually at high values, and slowed down gradually at intermediate values. However, as the length of the electrolysis increased, it quickly expanded. The consumption response of the outer anode as a function of the influent rate is shown in Figure 8c. The flow rates first climbed, then gradually declined.

More adsorbents are required at the start of the experiment because various ions are released from the electrodes at increasing pollutant concentrations. As a result, when there are too many adsorbents, the electrodes' dissolving rate is decreased. Due to the innovative electrode's current design's increased active area and the electrical conductivity of greasy wastewater, actual electrode consumption increased and eventually decreased. Anode degradation is slowed by the development of an oxide layer on its surface. According to [1] and [6], the same variables had a significant impact on electrode consumption.

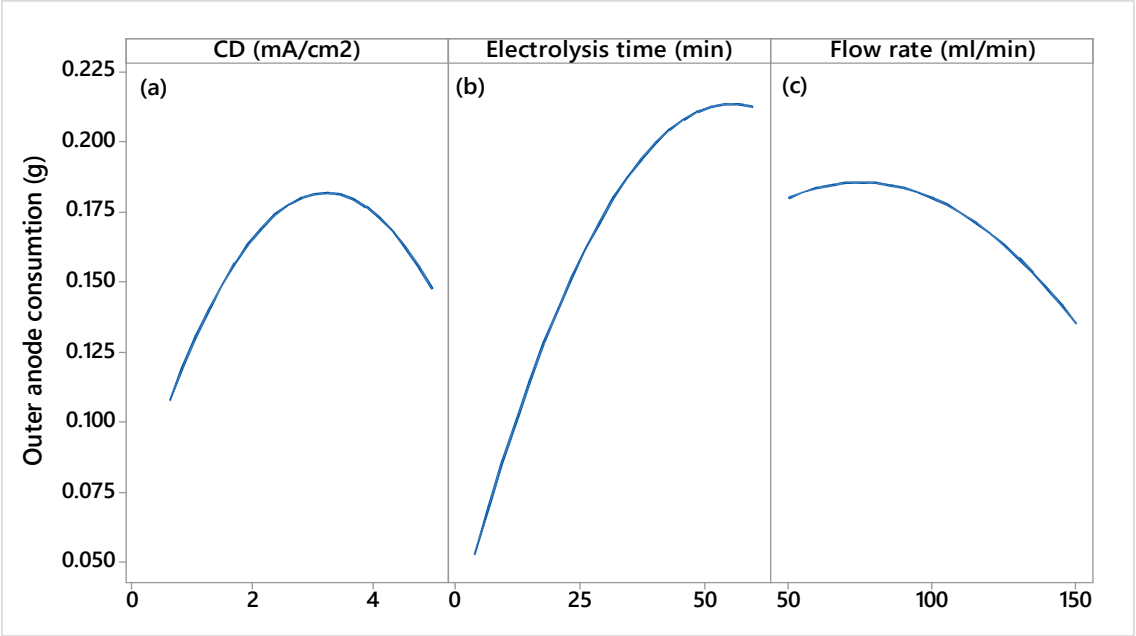

Figure 8: Operating parameter effects on outer-anode consumption. (a) CD (mA.cm^{-2}), (b) The treatment time (min), and (c) The influent rate (ml.min^{-1})

3.4 Effect of electrode consumption on TDS response

The final TDS response seen in Figure 9 will be evaluated in order to ascertain how inner and outer anode consumption impacts it. Figure 9 illustrates how the use of internal and external anodes and the final TDS response are related. An essential element of EC is electrode consumption; It regulates the pace at which ions released from the electrodes remove contaminants. The findings show that consumption of the outer electrode has a greater impact on the final TDS value than consumption of the inner electrode because the outside electrode has a larger surface area, which makes it simpler for a larger amount of hydroxide to be released. After that, the aluminum ion interacts with this hydroxide to create a considerable amount of adsorbent that can be used to remove pollutants from a solution.

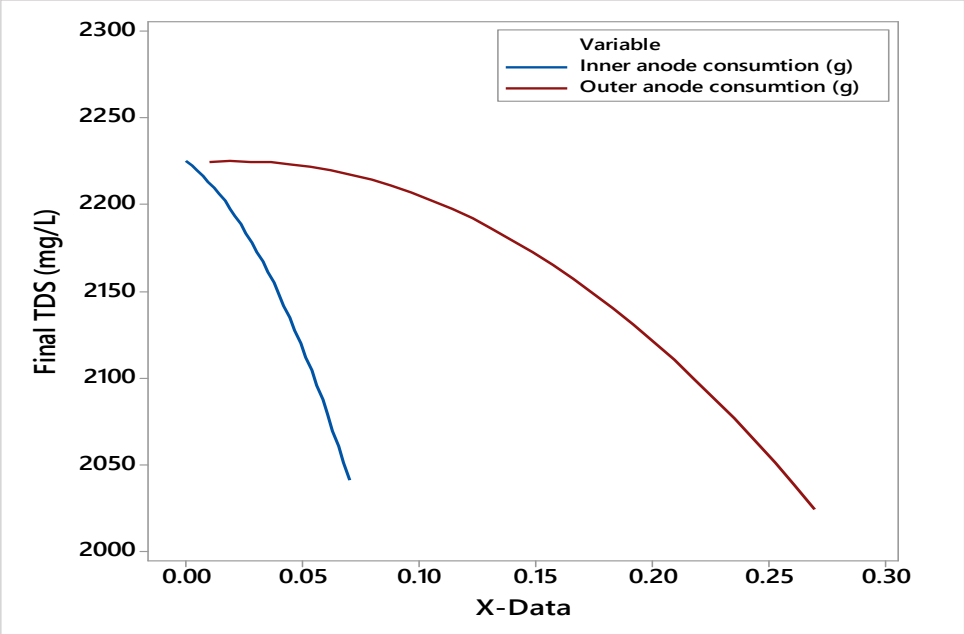

Figure 9: The effect of the final TDS reaction on the consumption of the inner and outer anodes

Figure 10 illustrates how the pair of internal and external anode consumption significantly affects the TDS response during the period of EC operation. The ultimate TDS response pattern seen in Figure 3d (10) indicates that the final TDS value will drop when electrode consumption rises since both anode consumption significantly affects the TDS value. These results fit the ANOVA results listed in Table 5 precisely.

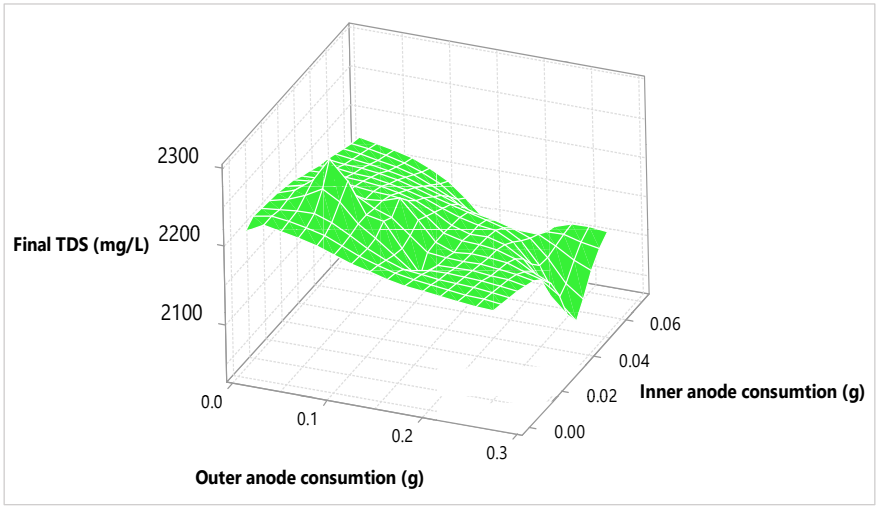

Figure 10: Consumption of anodes on the final TDS

Based on the testing data, Equations 7 and 8 indicate correlations for both anode consumption, respectively:
Consumption of inner-anode:

$$Y = -0.0159 - 0.00644\ X1 + 0.001361\ X2 + 0.000503\ X3 - 0.00032\ X12 - 0.000011\ X22 - 0.000003\ X32 +$$

$$0.000204\ X1*X2 + 0.000046\ X1*X3 - 0.000005\ X2*X3 \qquad (R^2=0.8995\ ;\ R^2_{Adj}=0.7187) \qquad (7)$$

Consumption of outer anode:

$$Y= -0.1377 + 0.0539\ X1 + 0.00556\ X2 + 0.00126\ X3 - 0.00716\ X12 - 0.000018\ X22 - 0.000003\ X32 + 0.000163\ X1*X2 - 0.000114\ X1*X3 - 0.000027\ X2*X3 \quad (R2=0.9664\ ;\ R2Adj=0.9059) \tag{8}$$

The high regression coefficient values of R2 of Equations 7 and 8 show that the model fits the data well and is consistent with their (R2 -adj) values.

Operational parameter optimization: Statistical software (Minitab-18) facilitated the evaluation of optimization phases. Achieving a feedback accuracy of 1, as depicted in Table 6, ensured precision in acquired data. Following an hour of treatment at a CD of 5.0 mA/cm^2 and an influent rate of 50 ml/min, the final TDS was minimized to 2000.45 mg/l. The study's key findings emphasized the efficacy of the newly developed EC reactor in removing TDS from petroleum wastewater. Larger fins exhibited a favorable influence, resulting in improved process variables, notably electrolysis duration and current density, compared to previous research. Table 7 provides a comparative value between the present study and those found in previous studies.

Table 6: The optimum conditions of the studied variables

Responses	Value
CD (mA/cm^2)	5
Final TDS (mg/L)	2000
Outer anode consumption (g)	0.63
Inner anode consumption (g)	0.45
Electrolysis time (min)	60
Flow rate (ml.min^{-1})	50

Table 7: A comparison between the present findings and some previous studies for TDS minimizing in wastewater

Optimal conditions	Removal efficiency	Ref.
40 A/m^2 and 20 min	49.78%	[45]
Six electrodes with 2000 mA current flow for 90 min	99%	[46]
5.5-27.8 mA/cm^2 and 30 min	Limited removal of TDS	[47]
1.625 A and 40 min	17.5%	[48]
60 min, 1 A, and 50 rpm	20%	[49]
75 rpm, 10 min, 4 L/min, 2 mA/cm^2, pH 8, 1 cm2, and 0.25 L/min	92.3%	[50]
pH 4, 60 min, 5 mA/cm^2	78%	[51]

4. Conclusion

Experiments were conducted on the effluent from the Al-Muthanna petroleum refinery to assess the efficacy of the state-of-the-art EC system in TDS removal. Optimal conditions of 50 ml/min flow rate, 5 mA/cm^2 current density, and 1-hour reaction time were determined. Consistent with previous findings, electrolysis time and current density emerged as critical factors influencing TDS elimination. Enhanced TDS removal was observed with increased current density (up to 5 mA/cm^2) and reaction time (up to 1 hour). Conversely, TDS removal decreased with higher flow rates. Notably, external electrode consumption had a more pronounced effect on final TDS values than internal electrode consumption. ANOVA data analysis and a high regression coefficient (R2 = 99.75%) affirm the accuracy of the updated predictive model. These findings unequivocally establish the reliability of the modern EC device for the remediation of petroleum effluent. The present innovative electrocoagulation reactor could be used as a pre-treatment process in addition to other treatment technologies, such as membrane technologies.

Acknowledgment

Acknowledgments may be directed to individuals or institutions that have contributed to the research or a government agency.

Author contributions

Conceptualization, **F. AlJaberi** and **M. Jasim**; data curation, **S. Alardhi**; formal analysis, **A. Salman**; investigation, **M. Jasim** and **F. AlJaberi**; methodology, **F. AlJaberi**; project administration, **F. AlJaberi**, **S. Alardhi**, resources, **F. AlJaberi**, **S. Alardhi**, **M. Jasim, A.Vargas, A. Salman** and **I. Cretescu** ; software, **M. Hathal**; supervision, **F. AlJaberi**; validation, **F. AlJaberi**, **S. Alardhi** and **A. Salman**; visualization, **I. Cretescu**; writing—original draft preparation, **M. Jasim**; writing—review and editing, **F. AlJaberi** and **A.Vargas**. All authors have read and agreed to the published version of the manuscript.

Funding

This research received no specific grant from any funding agency in the public, commercial, or not-for-profit sectors.

Data availability statement

The data that support the findings of this study are available on request from the corresponding author.

Conflicts of interest

The authors declare that there is no conflict of interest.

References

[1] M. A. Jasim, F. Y. AlJaberi, A. D. Salman, S. M. Alardhi, P-C Le, et al., Studying the effect of reactor design on the electrocoagulation treatment performance of oily wastewater, Heliyon, 9 (2023) e17794. https://doi.org/10.1016/j.heliyon.2023.e17794

[2] N. M. Jabbar, S. M. Alardhi, SM, Al-Jadir T, H. A. Dhahad, Contaminant removal from real refinery wastewater is associated with energy generation in microbial fuel cells. J. Ecol. Eng., 24 (2023) 107-114. https://doi.org/10.12911/22998993/156081

[3] N. M. Jabbar, S. M. Alardhi, A. K. Mohammed, I. K. Salih, T. M. Albayati, Challenges in the implementation of bioremediation processes in petroleum-contaminated soils: A review, Environ. Nanotechnol. Monit. Manage., 18 (2022) 100694. https://doi.org/10.1016/j.enmm.2022.100694

[4] F. Y. AlJaberi, Treatment of refinery wastewater by chemical advanced oxidation processes (UV-photolysis, fenton, and photo-fenton): a comparative study. Iran. J. Chem. Chem. Eng., 42 (2023) 2392-2833. https://doi.org/10.30492/ijcce.2023.560200.5520

[5] S. M. Alardhi, N. M. Jabbar, T. Al-Jadir, N. K. Ibrahim, A. M. Dakhil, N. D. Al-Saedi, et al., Artificial neural network model for predicting the desulfurization efficiency of Al-Ahdab crude oil, AIP Conf. Proc., 2443 (2022) 030033. https://doi.org/10.1063/5.0091975

[6] S. M. Alardhi, T. Al-Jadir, A. H. Hasan, A.A. Jaber, L. M. Al Saedi, Design of artificial neural network for prediction of hydrogen sulfide and carbon dioxide concentrations in a natural gas sweetening plant. Ecol. Eng. Environ. Technol., 24 (2023) 55-66. https://doi.org/10.12912/27197050/157092

[7] L. Tjale L, H. Richards, O. Mahlangu, L. N. Nthunya, Silica nanoparticle modified polysulfone/polypropylene membrane for separation of oil-water emulsions, Results Eng., 16 (2022) 100623. https://doi.org/10.1016/j.rineng.2022.100623

[8] A. Kadier, Z. Al-Qodah, G. K. Akkaya, D. Song, et al., A state-of-the-art review on electrocoagulation (EC): An efficient, emerging, and green technology for oil elimination from oil and gas industrial wastewater streams, Case Stud. Chem. Environ. Eng., 6 (2022) 100274. http://dx.doi.org/10.1016/j.cscee.2022.100274

[9] M. A. Jasim, F. Y. AlJaberi, Treatment of oily wastewater by electrocoagulation technology: A general review (2018-2022), J. Electrochem. Sci. Eng., 13 (2023) 361-372. https://doi.org/10.5599/jese.1472

[10] B. Diya'uddeen, W. Daud, A. R. Aziz, Treatment technologies for petroleum refinery effluents: A review, Process Saf. Environ. Prot., 89 (2011) 95-105. https://doi.org/10.1016/j.psep.2010.11.003

[11] M. A. Jasim, F. Y. AlJaberi, Investigation of oil content removal performance in real oily wastewater treatment by electrocoagulation technology: RSM design approach, Results Eng., 18 (2023) 101082. https://doi.org/10.1016/j.rineng.2023.101082

[12] M. H. El-Naas, S. Al-Zuhair, A. Al-Lobaney, S. Makhlouf, Assessment of electrocoagulation for the treatment of petroleum refinery wastewater, J. Environ. Manage., 91 (2009) 180-185. https://doi.org/10.1016/j.jenvman.2009.08.003

[13] M. Changmai, M. Pasawan, M. K. Purkait, Treatment of oily wastewater from drilling site using electrocoagulation followed by microfiltration, Sep. purify. Technol., 210 (2019) 463-472. https://doi.org/10.1016/j.seppur.2018.08.007

[14] T. K. Hussein, N. A. Jasim, A comparison study between chemical coagulation and electro-coagulation processes for the treatment of wastewater containing reactive blue dye, Mater. Today: Proc., 42 (2021) 1946-1950. https://doi.org/10.1016/j.matpr.2020.12.240

[15] D. D. Nguyen, H. H. Ngo, Y. S. Yoon, A new hybrid treatment system of bioreactors and electrocoagulation for superior removal of organic and nutrient pollutants from municipal wastewater, Bioresour. Technol., 153 (2014) 116-125. https://doi.org/10.1016/j.biortech.2013.11.048

[16] M. A. Jasim, F. Y. AlJaberi, P-C. Le, A. D. Salman, J. Miklos, B. Van, et al., Investigating the influences of the cathode configuration on the electrocoagulation performance: A comparative study, Case Stud. Chem. Environ. Eng., 8 (2023) 100364. https://doi.org/10.1016/j.cscee.2023.100364

[17] M. A. Jasim, F. Y. AlJaberi, Removal of COD from real oily wastewater by electrocoagulation using a new configuration of electrodes, Environ. Monit. Assess., 195 (2023). https://doi.org/10.1007/s10661-023-11257-y

[18] G. Barzegar, J. Wu J, Ghanbari F. Enhanced treatment of greywater using electrocoagulation/ozonation: Investigation of process parameters, Process Saf. Environ. Prot., 121 (2019) 125-132. https://doi.org/10.1016/j.psep.2018.10.013

[19] N. Karimi, S. A. Mirbagheri, R. Nouri, A. Bazargan, Sequential application of aerated electrocoagulation and γ-Fe_2O_3 nanoparticle adsorption for COD removal: Consuming the least amount of energy and economic evaluation, Results Eng., 17 (2023) 100770. https://doi.org/10.1016/j.rineng.2022.100770

[20] R. Raj, A. Tripathi, S. Das, M. M. Ghangrekar, Removal of caffeine from wastewater using electrochemical advanced oxidation process: A mini review, Case Stud. Chem. Environ. Eng., 4 (2021) 100129. https://doi.org/10.1016/j.cscee.2021.100129

[21] F. Y. AlJaberi, S. M. Alardhi, S. A. Ahmed, A. D. Salman, T. Juzsakova, I. Cretescu, et al., Can electrocoagulation technology be integrated with wastewater treatment systems to improve treatment efficiency? Environ. Res., 214 (2022) 113890. https://doi.org/10.1016/j.envres.2022.113890

[22] O. Ganzenko, D. Huguenot, V. Hullebusch, G. Esposito, M. A. Oturan, Electrochemical advanced oxidation and biological processes for wastewater treatment: a review of the combined approaches, Environ. Sci. Pollut. Res., 21 (2014) 8493-524. https://doi.org/10.1007/s11356-014-2770-6

[23] C. V. Nachiyar, A. D. Rakshi, S. Sandhya, N. Britlin, J. Nellore, Developments in treatment technologies of dye-containing effluent: A review, Case Stud. Chem. Environ. Eng., 7 (2023) 100339. https://doi.org/10.1016/j.cscee.2023.100339

[24] H. Faraj, A. Jamrah, S. Al-Omari S, T. Al-Zghoul, Optimization of an electrocoagulation-assisted adsorption treatment system for dairy wastewater, Case Stud. Chem. Environ. Eng., 9 (2024) 100574. https://doi.org/10.1016/j.cscee.2023.100574

[25] F. Y. AlJaberi, S. A. Ahmed, H. F. Makki, A. S. Naje, H. M. Zwain, A. D. Salman, et al., Recent advances and applicable flexibility potential of electrochemical processes for wastewater treatment, Sci. Total Environ., 867 (2023) 161361. https://doi.org/10.1016/j.scitotenv.2022.161361

[26] M. M. Jiad, A. H. Abbar, Treatment of petroleum refinery wastewater by an innovative electro-Fenton system: Performance and specific energy consumption evaluation, Case Stud. Chem. Environ. Eng., 8 (2023) 100431, https://doi.org/10.1016/j.cscee.2023.100431

[27] H. P. Carvalho, J. Huang, M. Zhao, G. Liu, L. Dong, X. Liu, Improvement of Methylene Blue removal by electrocoagulation/banana peel adsorption coupling in a batch system, Alexandria Eng. J., 54 (2015) 777-786. https://doi.org/10.1016/j.aej.2015.04.003

[28] Y. Liu, S.Lo, Y. Liou, Ch. Hu, Removal of nonsteroidal anti-inflammatory drugs (NSAIDs) by electrocoagulation–flotation with a cationic surfactant, Sep. Purif. Technol., 152 (2015) 148-154. https://doi.org/10.1016/j.seppur.2015.08.015

[29] F. Y. Al Jaberi, S. M. Jabbar, N. M. Jabbar, Modeling of adsorption isotherms of oil content through the electrocoagulation treatment of real oily wastewater. AIP Conf. Proc., 2213 ,2020, 020041. https://doi.org/10.1063/5.0000157

[30] D. D. Nguyen, H. H. Ngo, W. Guo, T. T. Nguyen, Et al., Can electrocoagulation process be an appropriate technology for phosphorus removal from municipal wastewater? Sci. Total Environ., 563-564 (2016) 549-556. https://doi.org/10.1016/j.scitotenv.2016.04.045

[31] T. Al-Jadir, S. M. Alardhi, M. A. Alheety, A. A. Najim, I. K. Salih, M. Al-Furaiji, et al., Fabrication and characterization of polyphenylsulfone/titanium oxide nanocomposite membranes for oily wastewater treatment, J. Ecol. Eng., 23 (2022)1-13 https://doi.org/10.12911/22998993/154770

[32] L. S. Pérez, O. M. Rodriguez, S. Reyna, J. L. Sánchez-Salas, J. D. Lozada, et al., Oil refinery wastewater treatment using coupled electrocoagulation and fixed film biological processes, Phys. Chem. Earth., Parts A/B/C , 91 (2016) 53-60. https://doi.org/10.1016/j.pce.2015.10.018

[33] D. D. Nguyen, Y. S. Yoon, H. H. Ngo, X. T. Bui, S. S. Kim, et al., Influences of operational parameters on phosphorus removal in batch and continuous electrocoagulation process performance, Environ. Sci. Pollut. Res. Int., 24 (2017) 25441-25451. https://doi.org/10.1007/s11356-017-0180-2

[34] F. Y. AlJaberi, Z.Y. Hawaas, Electrocoagulation removal of Pb, Cd, and Cu ions from wastewater using a new configuration of electrodes, MethodsX, 10 (2023) 101951. http://dx.doi.org/10.1016/j.mex.2022.101951

[35] J. Y. Wang, A. Kadier, J. M. Peralta-Hernández, C. G. Liang, P. C. Ma, An electrocoagulation (EC) process with a novel edge insulated electrode for separation of oil-in-water emulsions, Case Stud. Chem. Environ. Eng., 7 (2023) 100354. https://doi.org/10.1016/j.cscee.2023.100354

[36] F. Ghanbari, M. Moradi, A comparative study of electrocoagulation, electrochemical Fenton, electro-Fenton and peroxi-coagulation for decolorization of real textile wastewater: electrical energy consumption and biodegradability improvement, J. Environ. Chem. Eng., 3 (2015) 499-506. https://doi.org/10.1016/j.jece.2014.12.018

[37] Z. A. Hawass, F. Y. AlJaberi, Effect of mono and bipolar connection modes on the electrocoagulation removal efficiency of multi-heavy metals from simulated wastewater, Al-Qadisiyah J. Eng. Sci., 15 (2022) 48-54. http://dx.doi.org/10.30772/qjes.v15i1.813

[38] E. Gatsios, J. Hahladakis, E. Gidarakos, Optimization of electrocoagulation (EC) process for the purification of a real industrial wastewater from toxic metals, J. Environ. Manag., 154 (2015) 117-27. https://doi.org/10.1016/j.jenvman.2015.02.018

[39] S. Elabbas, N. Ouazzani, L. Mandi, F. Berrekhis, M. Perdicakis, S. Pontvianne, et al., Treatment of highly concentrated tannery wastewater using electrocoagulation: Influence of the quality of aluminium used for the electrode, J. Hazard. Mater., 319 (2016) 69-77. https://doi.org/10.1016/j.jhazmat.2015.12.067

[40] C. Tsioptsias, D. Petridis, N. Athanasakis, I. Lemonidis, A. Deligiannis, P. Samaras, Post-treatment of molasses wastewater by electrocoagulation and process optimization through response surface analysis, J. Environ. Manag., 164 (2015) 104-113. https://doi.org/10.1016/j.jenvman.2015.09.007

[41] V. Kuokkanen, T. Kuokkanen, J. Rämö, U. Lassi, J. Roininen, Removal of phosphate from wastewaters for further utilization using electrocoagulation with hybrid electrodes–Techno-economic studies, J. Water Process Eng., 8 (2015) e50-e7. https://doi.org/10.1016/j.jwpe.2014.11.008

[42] T. J. Mohammed, H. A. Al-Zuheri, Application of response surface methodology for analysis and optimization of the operational parameters for turbidity removal from oily wastewater by electrocoagulation process. IOP Conference Series, Mater. Sci. Eng., 454 , 2018, 012069. https://doi.org/10.1088/1757-899X/454/1/012069

[43] J. Schaep, B. V. Bruggen, S. Uytterhoeven, R. Croux, C. Vandecasteele, et al., Removal of hardness from groundwater by nanofiltration, Desalination 119 (1998) 295-301. https://doi.org/10.1016/S0011-9164(98)00172-6

[44] W. Jiang, Y. Chen, M. Chen, X. Liu, Y. Liu, T. Wang, et al., Removal of emulsified oil from polymer-flooding sewage by an integrated apparatus including EC and separation process, Sep. Purif. Technol., 211 (2019) 259-68. https://doi.org/10.1016/j.seppur.2018.09.069

[45] C. J. Nawarkar, V. D. Salkar, Solar powered Electrocoagulation system for municipal wastewater treatment, Fuel, 237 (2019) 222-226. https://doi.org/10.1016/j.fuel.2018.09.140

[46] S. Jose, L. Mishra, S. Debnath, S. Pal, G. Basu, Improvement of water quality of remnant from chemical retting of coconut fibre through electrocoagulation and activated carbon treatment, J. Cleaner Prod., 210 (2019) 630-637. https://doi.org/10.1016/j.jclepro.2018.11.011

[47] S. Kamyar, P. Fyfe, S. R. Wickramasinghe, Integrated electrocoagulation – Forward osmosis – Membrane distillation for sustainable water recovery from hydraulic fracturing produced water, J. Membr. Sci., 574 (2019) 325-337. https://doi.org/10.1016/j.memsci.2018.12.075

[48] F. Y. AlJaberi, S. A. Ahmed, H. F. Makki, Electrocoagulation treatment of high saline oily wastewater: evaluation and optimization, Heliyon, 6 (2020) e03988. https://doi.org/10.1016/j.heliyon.2020.e03988

[49] R. F. Abbass, A. A. Amooey, F. Y. AlJaberi, Electrocoagulation removal of COD and TDS from real municipal wastewater sourced from the Euphrates River using multipole arrangement, Results Chem., 9 (2024) 101613. https://doi.org/10.1016/j.rechem.2024.101613

[50] A. A. Abbas, M. M. Hanafiah, SO42−, Cl−, Br−, and TDS removal by semi continuous electrocoagulation reactor using rotating anode, Environ. Technol. Innovation, 28 (2022) 102917. https://doi.org/10.1016/j.eti.2022.102917

[51] S. A. Bakry, M. E. Matta, K. Zaher, Electrocoagulation process performance in removal of TOC, TDS, and turbidity from surface water, Desalin. Water Treat., 129 (2018) 127-138. https://doi.org/10.5004/dwt.2018.23070